

Do non-relativistic neutrinos constitute the dark matter?

THEO M. NIEUWENHUIZEN^(a)

Institute for Theoretical Physics, University of Amsterdam, Valckenierstraat 65, 1018 XE Amsterdam, The Netherlands

PACS 95.35.+d – Dark matter

PACS 98.65.-r – Galaxy groups, clusters, and superclusters

PACS 14.60.St – Non-standard-model neutrinos, right-handed neutrinos, etc.

Abstract. - The dark matter of the Abell 1689 galaxy cluster is modeled by thermal, non-relativistic gravitating fermions and its galaxies and X-ray gas by isothermal distributions. A fit yields a mass of $h_{70}^{1/2} (12/\bar{g})^{1/4} 1.445 (30)$ eV. A dark matter fraction $\Omega_\nu = h_{70}^{-3/2} 0.1893 (39)$ occurs for $\bar{g} = 12$ degrees of freedom, i. e., for 3 families of left plus right handed neutrinos with masses $\approx 2^{3/4} G_F^{1/2} m_e^2$. Given a temperature of 0.045 K and a de Broglie length of 0.20 mm, they establish a quantum structure of several million light years across, the largest known in the Universe. The virial α -particle temperature of 9.9 ± 1.1 keV/ k_B coincides with the average one of X-rays. The results are compatible with neutrino genesis, nucleosynthesis and free streaming. The neutrinos condense on the cluster at redshift $z \sim 28$, thereby causing reionization of the intracluster gas without assistance of heavy stars. The baryons are poor tracers of the dark matter density.

Introduction. – Dark matter is postulated by Oort to explain the motion and density of stars perpendicular to the Galactic plane [1]. Zwicky points out that galaxy clusters must contain dark matter, [2] while Rubin demonstrates that galaxies require dark matter in order to explain the rotation curves of stars and hydrogen clouds [3]. Nowadays, gravitational lensing observation is standardized, and dark matter filaments on the scale of clusters of galaxies between empty voids can be inferred [4].

The main dark matter candidates are Massive Astrophysical Compact Halo Objects (MACHOs), Weakly Interacting Massive Particles (WIMPs), elementary particles, and further, e. g., axions. Of the total mass of the universe, $\Omega_B = 0.0227/h^2 \approx 4.23\%$ consists of baryons, of which a minor part is luminous, a part is located in gas clouds, and a part makes up the galactic dark matter as MACHOs [5–7]. However, the remaining mass of the universe is non-baryonic, dark energy and dark matter. The dark matter, with cosmic fraction $\Omega_D = 21.4 \pm 2.7\%$ according to WMAP5 [8], will be the focus of the present work, where we assume it to consist of fermionic WIMPs.

Thermal fermion model. – We consider non-interacting dark fermions (x) with mass m and \bar{g} degrees of freedom, subject to a spherically symmetric gravitational potential $U(r)$ and in equilibrium at temperature T . The mass density reads

$$\rho_x = \int \frac{d^3p}{(2\pi\hbar)^3} \frac{\bar{g}m}{\exp[(p^2/2m + mU(r) - \mu)/k_B T] + 1}, \quad (1)$$

where \mathbf{p} is the momentum and $\mu = \alpha k_B T$ the chemical potential. The spherically symmetric potential normalized at $U(0) = 0$ reads $U(r) = G \int d^3r' \rho(r') (1/r' - 1/|\mathbf{r} - \mathbf{r}'|)$. It satisfies the Poisson equation $U'' + 2U'/r = 4\pi G\rho$. In dimensionless variables, $x = r/R_*$, $\phi = mU/k_B T$, one has

$$\rho_x(r) = -\frac{\bar{g}m}{\lambda_T^3} \text{Li}_{3/2} \left(-e^{\alpha - \phi(x)} \right), \quad (2)$$

with the polylogarithm $\text{Li}_\gamma(z) = \sum_{k=1}^{\infty} z^k/k^\gamma$ for $|z| < 1$ and analytically continued elsewhere. The thermal wavelength λ_T and a characteristic scale R_* read, respectively,

$$\lambda_T = \left(\frac{2\pi\hbar^2}{mk_B T} \right)^{1/2}, \quad R_* = \left(\frac{\lambda_T^3 k_B T}{4\pi\bar{g}Gm^2} \right)^{1/2}. \quad (3)$$

Accounting also for the galaxies (G) and the hot X-ray gas (g), see below, the Poisson equation will take the form

$$\phi'' + \frac{2}{x}\phi' = -\text{Li}_{3/2} \left(-e^{\alpha - \phi} \right) + e^{\alpha_G - \bar{\beta}_G \phi} + e^{\alpha_g - \bar{\beta}_g \phi}. \quad (4)$$

For $\alpha \rightarrow -\infty$ it reduces to a two component isothermal model, that describes galaxy rotation curves well; for $\alpha_G, \alpha_g \rightarrow -\infty$ it becomes the fermionic isothermal model.

^(a)t.m.nieuwenhuizen@uva.nl

The total mass inside a sphere of radius $r = R_*x$ reads

$$M(r) = \frac{k_B T R_*}{Gm} x^2 \phi'(x). \quad (5)$$

Abell 1689. – This is the best studied galaxy cluster, known for its large lensing arcs, notably one at the Einstein radius $r_E = 50''$. It is well relaxed and spherically symmetric, with an intruding subcluster in the North-East, which does not affect the South-West hemisphere. It offers a test for the above. From gravitational lensing the azimuthally averaged mass profile is deduced, [9]

$$\Sigma(r_\perp) = \int_{-\infty}^{\infty} dz \rho \left(\sqrt{r_\perp^2 + z^2} \right). \quad (6)$$

The average redshift is $z = 0.183$. Observations are presented up to $r_m = h^{-1}$ Mpc, with Hubble constant $H_0 = 100h$ km/s Mpc. Relatively small fluctuations occur in the contrast function $\Delta\bar{\Sigma}(r)$ of the averaged Σ within r versus outside r . The first piece reads

$$\bar{\Sigma}(r) = \frac{1}{\pi r^2} \int_0^r dr_\perp 2\pi r_\perp \Sigma(r_\perp) \equiv \frac{1}{\pi r^2} M_{2D}(r). \quad (7)$$

The average between r and r_m is directly related to this, $\bar{\Sigma}(r \rightarrow r_m) = [M_{2D}(r_m) - M_{2D}(r)]/[\pi(r_m^2 - r^2)]$, so

$$\Delta\bar{\Sigma}(r) \equiv \bar{\Sigma}(r) - \bar{\Sigma}(r \rightarrow r_m) = \frac{\bar{\Sigma}(r) - \bar{\Sigma}(r_m)}{1 - r^2/r_m^2}. \quad (8)$$

From (7) and (6) one derives

$$\bar{\Sigma}(r) = \frac{4}{r^2} \int_0^\infty dr' r' \rho(r') \left[r' - \Re \left(\sqrt{r'^2 - r^2} \right) \right]. \quad (9)$$

After defining an amplitude $A \equiv \hbar^6/2\bar{g}^2 G^3 m^8 R_*^5$, eliminating T via (3), $T = \pi \hbar^6/2\bar{g}^2 G^2 k_B m^7 R_*^4$, and using (4), also $\bar{\Sigma}$ can be expressed in terms of ϕ' ,

$$\bar{\Sigma}(r) = A \Phi \left(\frac{r}{R_*} \right), \quad \Phi(x) = \int_0^\infty ds \phi'(x \cosh s). \quad (10)$$

To proceed, we consider the baryonic matter, galaxies (G) and, mostly, a hot X-ray gas (g). In hydrostatic equilibrium, $p'_i/\rho_i = -GM(r)/r^2$, ($i = x, G, g$), both the classical galaxies and the low density gas have a Boltzmann distribution, $\rho_G \sim \exp(-U/\sigma_v^2)$ with σ_v the line-of-sight velocity dispersion and $\rho_g \sim \exp(-\beta_g \bar{m}_g U)$ with $\bar{m}_g = 0.609 m_N$ the average mass in the gas.¹ Hydrostatic equilibrium then imposes $\beta_g = 1/k_B T_g$ where T_g is the gas temperature. With $\beta_G = k_B T/m\sigma_v^2$ and $\bar{\beta}_g = \bar{m}_g T/mT_g$,

¹For typical 0.3 solar metallicity one has $n_H = 10 n_{\text{He}}$, so $p_g = 2.3 n_H k_B T_g$, $\rho_g = 1.4 n_H m_N$ and $\bar{m}_g/m_N = 1.4/2.3$.

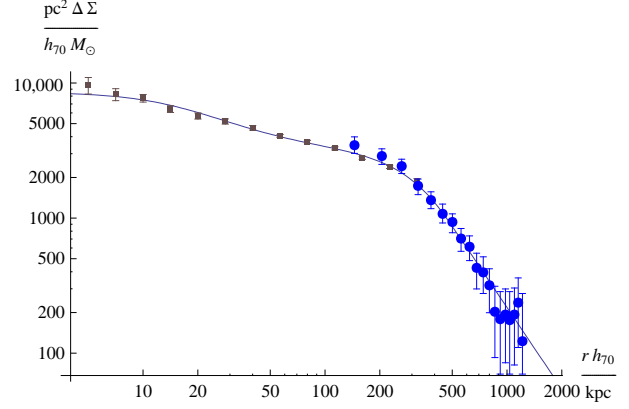


Fig. 1: The mass contrast $\Delta\bar{\Sigma}$ as function of radius r . Large data points from Ref. [9], small ones (at radii $5 \cdot 2^n/2 \cdot h_{70}^{-1}$ kpc with $n = 0, \dots, 12$) constructed from Fig. 6 of Ref. [10]. Full line: The theoretical profile; it softens below 7 kpc.

the densities may be written as $\rho_i \equiv \bar{g} m \lambda_T^{-3} \exp(\alpha_i - \bar{\beta}_i \phi)$, ($i = G, g$). This leads to the last two terms of Eq. (4).

We can now make a χ^2 fit of Eqs. (8) and (10) to the 19 data points of [9], combined with 13 points constructed from recent core values for $M_{2D}(r)$ [10] and $\bar{\Sigma}(r_m)$ from our model. As seen in Fig. 1, the relative errors increase strongly with r , which reduces the effective number of points. The errors become more equal if we consider the χ^2 of $\sqrt{\Delta\bar{\Sigma}}$. As explained later, we take $\bar{\beta}_g = 0.153$ and $\alpha_g = 2.36$ at $\bar{\beta}_G = 1$. There is a minimum $\chi^2 = 13.617$ at $\bar{\beta}_G = 0.80$. This is close to the virialized value $\bar{\beta}_G = 1$, so we stick to that with its $\chi^2 = 13.645$. With $h \equiv 0.70 h_{70}$, the correlation matrix for the upper errors yields

$$\begin{aligned} A &= 59.4 \pm 9.6 h_{70} M_\odot \text{pc}^{-2}, & \alpha &= 38.4 \pm 3.1, \\ R_* &= 297 \pm 10 h_{70}^{-1} \text{kpc}, & \alpha_G &= 8.26 \pm 0.32. \end{aligned} \quad (11)$$

We present its fit in Figure 1. The WIMP mass reads

$$m = \frac{1}{2^{1/8} \bar{g}^{1/4}} \frac{\hbar^{3/4}}{G^{3/8} A^{1/8} R_*^{5/8}}. \quad (12)$$

Since $AR_*^5 = 136 \pm 25 h_{70}^{-4} M_\odot \text{Gpc}^3$, m has a 2% error,

$$m = h_{70}^{1/2} \left(\frac{12}{\bar{g}} \right)^{1/4} 1.455 \pm 0.030 \text{ eV}. \quad (13)$$

With $T_{\gamma 0} = 2.725$ K, the global fermion density is

$$n_F = g \frac{3}{4} \frac{4}{11} \frac{\zeta(3)}{\pi^2} \left(\frac{k_B T_{\gamma 0}}{\hbar c} \right)^3 = g 55.977 \text{ cc}^{-1}. \quad (14)$$

While \bar{g} is the number of states that can be filled in the cluster formation process, g is the filling factor in the dark matter genesis. The global mass fraction thus reads

$$\Omega_x = \frac{n_F m}{\rho_c} = \frac{g}{12} \left(\frac{12}{\bar{g}} \right)^{1/4} h_{70}^{-3/2} 0.1893 \pm 0.0039. \quad (15)$$

The gravitino of supersymmetry ($s=3/2$, $\bar{g} = 8$) can explain the Abell data, but it decouples early, in the presence of $g_* \sim 100$ relativistic degrees of freedom, so that $g \sim 0.4$ leads to a small $\Omega_x \sim 0.8\%$. The same holds for other early decouplers [11]. Bosons, like the axion, can not fit the data because of the tilt in Fig. 1 at $r < 200$ kpc; axionic Bose-Einstein condensation can only exist up to the small scale $\sqrt{\lambda_T R_*}$, which is of no help.

Neutrinos. – They can occupy in the cluster formation process all $\bar{g} = 12$ left and righthanded states, which gives $m = 1.455(30) h_{70}^{1/2}$ eV. Neutrinos oscillate, [12] $\Delta m_{12}^2 = 8.0_{-0.3}^{+0.4} 10^{-5} \text{eV}^2$, $\Delta m_{23}^2 = 1.9 - 3.0 10^{-3} \text{eV}^2$ so the mass eigenvalues differ. It is natural to suppose that all virial speeds are equal, so $T_i = T m_i/m$. If also their chemical potentials behave as $\mu_i = k_B T_i \alpha$, the above approach still applies with $m = (m_1 + m_2 + m_3)/3$. The degeneracy parameter will change negligibly,

$$\bar{g} = \sum_{i=1}^{12} \frac{m_i^4}{m^4} = 12 + \mathcal{O} \left(\frac{(\Delta m_{23}^2)^2}{m^4} \right). \quad (16)$$

The oscillations bring a shift smaller than our error bars,

$$m_{1,2} = m - \frac{\Delta m_{23}^2}{6m} \mp \frac{\Delta m_{12}^2}{4m}, \quad m_3 = m + \frac{\Delta m_{23}^2}{3m}. \quad (17)$$

Sterile masses are expected to weigh keV's or more, see [13] for a review, but a (near) equality between left and right handed masses and their abundances is needed to maximize $\Omega_x \approx h_{70}^{-3/2} \frac{0.19}{12} \sum_{i=1}^{12} n_i m_i / \left(\frac{1}{12} \sum_{i=1}^{12} n_i m_i^4 \right)^{1/4}$.

The de Broglie length in the cluster $\lambda_{T\nu} = 2\bar{g}\hbar^{-2} Gm^3 R_*^2 = 0.20$ mm is visible to the human eye; the Compton length is 0.136μ . The A1689 neutrino temperature $T_\nu^A = \pi G m_\nu A R_* / k_B = 0.0447$ K is low and makes them strongly non-relativistic, with local dispersion

$$\sigma_\nu^v \equiv \left[\frac{\langle p_x^2 \rangle}{m^2} \right]^{1/2} = \left[\frac{\text{Li}_{5/2}(-e^{\alpha-\phi(r/R_*)})}{\text{Li}_{3/2}(-e^{\alpha-\phi(r/R_*)})} \right]^{1/2} \sigma_\nu^G, \quad (18)$$

which at large r equals the *galaxy* velocity dispersion $\sigma_\nu^G = \sqrt{k_B T/m} = 488 \pm 60$ km/s. The latter agrees reasonably with estimated speeds in [10] and with the 295 ± 40 km/s of the singular isothermal sphere that fits the mean galaxy distribution [14]. Indeed, between 5 and 80 kpc ρ_G looks somewhat like a singular isothermal distribution.

Neutrinos are abundant, see (14), but their speed is too low to leave traces such as Cherenkov radiation. Condensed in clusters, their local density is large. One has $n_\nu(0) = -\bar{g}\lambda_T^{-3} \text{Li}_{3/2}(-e^\alpha) = 2.3 10^8/\text{cc}$ and $\rho_\nu(0)c^2 =$

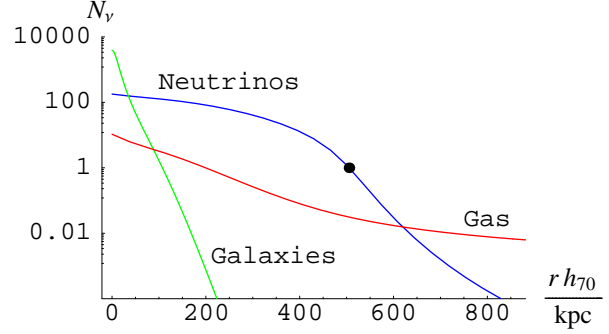


Fig. 2: Blue line: The neutrino number per cubic thermal length and per degree of freedom N_ν as function r . The point $(505 h_{70}^{-1} \text{kpc}, 1)$ separates the region $N_\nu > 1$ which exhibits strong quantum effects from the classical region $N_\nu \ll 1$. Green line: The galaxy mass density, at the same scale, is concentrated in the center. Red line: The gas mass density at the same scale.

0.34 GeV/cc , while $n_B(0) = 5.1 10^9/\text{cc}$. The quantum parameter $N_\nu(r) = -\text{Li}_{3/2}(-e^{\alpha-\phi})$ is plotted in Fig. 2. Its maximum is $N_\nu(0) = 180$, so quantum statistics is indispensable. We may define the quantum-to-classical transition by $N_\nu(r_{qc}) = 1$. This gives $r_{qc} = 505 h_{70}^{-1} \text{kpc}$ or diameter $3.3 10^6$ lyr, a giant size for quantum behavior.

As seen in Fig. 2, the baryons are poor tracers of the dark matter density, even they do trace the enclosed mass.

Neutrino free streaming (fs) in expanding space, $H(t) = \dot{a}/a$, is described by a collisionless Boltzmann equation,

$$\partial_t f_\nu + \frac{\mathbf{p} \cdot \partial_{\mathbf{r}} f_\nu}{m_\nu} - \left(\mathbf{p} H + \hat{\mathbf{r}} \frac{G m_\nu M(r, t)}{r^2} \right) \cdot \partial_{\mathbf{p}} f_\nu = 0. \quad (19)$$

Below the Compton temperature $T_\nu^C = 16,850$ K the distribution $f_\nu^{\text{fs}} = 1/(e^{p c/k_B T_\nu} + 1)$ is long maintained with sliding $T_\nu = (4/11)^{1/3} T_\gamma$, until the last, Newtonian term sets in. In the fs regime the scaling $p \sim k_B T_\nu/c$ implies

$$p_{\text{fs}} \equiv \sqrt{\langle p^2 \rangle_{\text{fs}}} = 2.567 \frac{k_B T_\gamma}{c}. \quad (20)$$

The neutrinos condense (νc) on the cluster when the typical Newton force $G m_\nu M(R_*)/R_*^2 = 6.56 10^{-10} m_\nu \text{ms}^{-2}$ becomes comparable to the free streaming force, $p_{\text{fs}} H = 2.82 10^{-13} m_\nu (z+1) \sqrt{\Omega_\Lambda + \Omega_M (z+1)^3} \text{ms}^{-2}$, which happens for $\Omega_M = 1 - \Omega_\Lambda = 0.25$ at $z_{\nu c} = 28.3$, $T_\gamma^{\nu c} = 77.2$ K and age 120 Myr. Consistency occurs by the near match of kinetic energies, $\frac{3}{2} m_\nu [\sigma_\nu^v(R_*)]^2 = 0.64 \times (p_{\text{fs}}^{\nu c})^2 / 2 m_\nu$. The free streaming stops then and the temperature sinks only moderately, from the cross over value $T_\nu^{A\nu c} = \frac{3}{2} m_\nu (\sigma_\nu^G)^2 / k_B = 0.13$ K to present one, $T_\nu^A = 0.0447$ K. Literature often mentions 1.95 K as present neutrino temperature; this derives from relativistic free streaming, but since they are non-relativistic, the kinetic temperature would even be lower, $T_\nu^{\text{kin}} = 2E_{\text{kin}}^{\text{fs}} / 3k_B = 9.6 10^{-4}$ K.

Our T_ν^A is higher because the condensation basically stops the cooling. The neutrino gas then clusters with a speed of sound $v_s^{\nu c} = \sqrt{5p/3\rho} = 2620$ km/s at the Jeans scale $L_{J\nu} = v_s^{\nu c}/\sqrt{G\rho_\nu^{\nu c}} = 1.57$ Mpc. The Jeans mass $M_{J\nu} = \pi\rho_\nu^{\nu c}L_{J\nu}^3/6 = 1.3 \cdot 10^{15} M_\odot$ estimates the total mass (5) at $r_m = 1$ Mpc/h, $M_{\text{tot}}(r_m) = 6.9 \cdot 10^{14} M_\odot$. Only 1.1% of this is in galaxies, and 1.5% in gas: the A1689 cluster is baryon poor, a property noticed before [9, 16].²

Virialization, gas profile and X-ray emission. – Partial thermalization takes place since during the condensation the individual objects, neutrinos, H, He and other gas atoms, and galaxies move in a time dependent gravitational potential, which changes each ones energy at a rate proportional to its mass. If the phase space occupation becomes uniform, a Fermi-Dirac distribution emerges [18] and our approach applies; else it yields an estimate.

This thermalization heats and reionizes the loosely bound parts of the intracluster gas. The virial proton temperature of the A1689 cluster, $T_p^A = m_p T_\nu^A/m_\nu = 2.48$ keV, has the order of magnitude of the average X-ray temperature 10.5 ± 0.1 keV of the cluster and the one of the South Western hemisphere, 11.1 ± 0.6 keV [15]. But virial equilibrium of the α -particles, at temperature $T_\alpha^A = m_\alpha T_\nu^A/m_\nu = 9.9 \pm 1.1$ keV, explains these observations. For this reason, we have already taken $\bar{\beta}_g = \bar{m}_g/m_\alpha$.

As expected theoretically, this gives a good match for the mass profile of the gas, which is deduced from the X-ray profile [16]. Fitting their first data point $M_g = 7.79 h^{-1} M_\odot$ at $30 h^{-1}$ kpc to our results sets $\alpha_g = 2.36$ at $h = 0.7$, as used above. Then the next 6 data points, up to $200 h^{-1}$ kpc, match within the symbol size with our theory. From there on, it underestimates the data, by a factor 4.5 at the last point at $716 h^{-1}$ kpc. Reasons for this may be a decay of the temperature beyond $200 h^{-1}$ kpc [16] and a contamination of the data from the more relaxed South West with those from the less relaxed North East.

The bolometric (total) energy emission $1.66 \pm 0.64 \cdot 10^{38}$ W [16] must be supplied by a slow contraction of the cluster. Thus the radiation serves to maintain the virial equilibrium state as it does for stars [19]. This will double the A1689 gravitational energy in some 700 Gyr.

Extended standard model and dark matter fraction. – Righthanded neutrinos have no hypercharge, so they justly do not enter the Z decay. Their mass is described as for quarks. The Yukawa eigenvalue $Y_{\nu_1} = 2^{3/4} G_F^{1/2} m_{\nu_1}$ can be expressed in the electron coupling $Y_e = 2.935 \cdot 10^{-6}$ as $Y_{\nu_1} = 0.966(20) h_{70}^{1/2} Y_e^2$. This exhibits some order in the lepton masses; in case $h_{70} = 1.062(42)$ or $h = 0.744(30)$ it implies

$$m_{\nu_1} = Y_e m_e = 2^{3/4} G_F^{1/2} m_e^2 = 1.4998 \text{ eV}. \quad (21)$$

²The missing baryons may be located in intercluster clouds, such as the observed 0.91 keV gas of mass $\sim 10^{14} M_\odot$ in a bridge between the 4.43 keV A222 cluster and the 5.31 keV A223 cluster [17].

Active neutrinos (lefthanded neutrinos, righthanded antineutrinos) have $g = 6$ degrees of freedom. Eq. (15) leads to a cosmic density $0.0952 \pm 0.0019 h_{70}^{-3/2}$, clearly exceeding the $0.028 h_{70}^{-2}$ of WMAP5 ($0.013 h_{70}^{-2}$ when combined with baryon acoustic oscillations and supernovas) [8].

The situation can be even more interesting, since the occupation of the (mostly) righthanded states (sterile neutrinos) can have become sizeable if there is also a Majorana mass matrix. The latter couples the neutrino to its charge conjugate, rather than to the antineutrino, see e. g. [20]. This allows neutrinoless double β -decay, where the two neutrinos emitted in the β decays annihilate each other, and the electrons leave with opposite momenta. For simplicity we consider the case of 6 sterile states, bringing the total number of neutrino states at $\bar{g} = 12$, the case discussed so far. In order to keep nearly equal masses, we need small Majorana terms M_i ($i = 1, 2, 3$ denotes the families), not the large ones of the see-saw mechanism. A one-family version of the problem shows that a (nearly) thermal occupation of sterile modes is possible above the decoupling temperature 3.5 MeV, provided $M_i > 3 \cdot 10^{-5} \text{ eV}^2/m_\nu \approx 2 \cdot 10^{-5} \text{ eV}$ [21]. Experimental searches have determined the upper bound $\frac{1}{2} M_e \approx m_{\beta\beta} < 0.2 - 0.7 \text{ eV}$ [22]. This filling implies that $g = 12$ can be reached, leading to a dark matter fraction

$$\Omega_\nu \leq 0.1904 \pm 0.0038 h_{70}^{-3/2}. \quad (22)$$

The case $g \approx \bar{g} > 12$ is also possible. For $g \sim 33$ it has enough matter to reach $t_0 \approx 1.0/H_0$ without dark energy.

Nucleosynthesis. – Our additional relativistic matter can be coded in the enhancement factor S [23], $\rho' = S^2 \rho$; after $e^+ - e^-$ freeze out it reads for $g = 12$

$$S = \left(\frac{16 + 7g(4/11)^{4/3}}{16 + 42(4/11)^{4/3}} \right)^{1/2} = 1.1854. \quad (23)$$

This enhances expansion, $H' = SH$, leaving less time for neutron decay and resulting in too much ${}^4\text{He}$. It can be balanced by a neutrino asymmetry due to a dimensionless chemical potential ξ , an effect which induces more n decays via $n + \nu_e \rightarrow p + e$,

$$L_e \equiv \frac{n_{\nu_e} - n_{\bar{\nu}_e}}{n_\gamma} = \frac{\pi^2}{12\zeta(3)} \left(\frac{T_\nu}{T_\gamma} \right)^3 (\xi + \frac{\xi^3}{\pi^2}). \quad (24)$$

With $\eta_{10} \equiv 10^{10} n_B/n_\gamma = 121 \Omega_B h_{70}^2$, the cosmic microwave background (CMB) value reads $\eta_{10}^{CMB} = 5.60 \pm 0.15$ [8]. The ${}^4\text{He}$ value $0.88_{-0.88}^{+3.75}$ does not fit to it, which motivated to put conservative error bars [23]. But the effects of extra matter and asymmetry on He are large,

$$\eta_{\text{He}} = \eta_{10} + 100(S - 1) - \frac{575}{4} \xi. \quad (25)$$

So we may fix ξ by matching to η_{10}^{CMB} . This yields $\xi = 0.162$, $L_e = 0.040$. Other authors report a ${}^4\text{He}$ value closer to the one of CMB [24], but this does not modify ξ much. For Li, $\eta_{\text{Li}} = 6.05_{-0.12}^{+0.13}$, a similar approach brings [23]

$$\eta_{10} = \eta_{\text{Li}} + 3(S - 1) + \frac{7}{4}\xi = 6.88_{-0.12}^{+0.13}, \quad (26)$$

while for deuterium, $\eta_D = 5.92_{-0.33}^{+0.30}$, it implies

$$\eta_{10} = \eta_D + 6(S - 1) - \frac{5}{4}\xi = 6.83_{-0.33}^{+0.30}. \quad (27)$$

The freedom in ξ appears to solve the ${}^4\text{He}$ discrepancy. Since the CMB value still has to be rederived for the prior of neutrino dark matter, the final result may end up near $\eta_{10} = 6.88 \pm 0.15$, $\Omega_B h_{70}^2 = 5.69 \pm 0.12\%$, to be compared with $\Omega_B h_{70}^2 = 4.63 \pm 0.12\%$ from WMAP5. Together with (22) it would lead to a total matter fraction $\Omega_M = \Omega_B + \Omega_\nu \approx 24.7 \pm 0.5\%$, while WMAP5 reports $25.8 \pm 3.0\%$.

Conclusion. — On the basis of three assumptions, Newton’s law, quantum statistics and virialization, we derive the profile of quantum particles (WIMPs), galaxies and intracluster gas. Because of the virialization — equal velocity dispersions for WIMPs, galaxies and α -particles, or, more precisely, each one’s temperature proportional to its mass — the WIMPs have a polylogarithmic profile, while the galaxies and the gas have isothermal profiles.

A fit to total (lensing) mass observations of the cluster Abell 1689 is possible only for fermionic WIMPs with eV mass. The error of this method is small, 2% for the present data set. Although we have not shown the validity of our virial equilibrium assumption, the explanation of the X-ray temperature of the hot gas, $T_g \sim 10 \text{ keV} = 116 \cdot 10^6 \text{ K}$, as the virial temperature of α -particles is striking. Due to collisions that temperature is shared by the electrons, protons and ions. The predicted mass profiles for galaxies and gas are also consistent with observations.

This suggests that our approach cannot be far off, so the WIMP mass is a few eV and dark matter is hot. Early decouplers that have been in equilibrium would yield a small cosmic dark matter fraction [11], so if they would set the dark matter of the A1689 cluster, there should also be other dark matter, the major part, but absent in this cluster, which is unlikely. Therefore early decouplers such as the gravitino are ruled out as dark matter candidates. The thermal axion is ruled out because it is a boson.

The case of $\bar{g} = 12$ degrees of freedom performs well, pointing at three families of left and right handed fermions and antifermions. The obvious candidate is the massive neutrino, because when condensed in the cluster the left and righthanded states are equally available. The mass is then $m_\nu = 1.445 h_{70}^{1/2} \text{ eV}$ with a 2% margin and smaller variations between the species due to neutrino oscillations. There is the striking connection $m_\nu \sim 2^{3/4} G_F^{1/2} m_e^2$. The dark matter fraction of active neutrinos is then 9.5%,

showing that the cold dark matter analysis, that allows only 1.3% at best [8], must definitively be erroneous.

The scenario in which dark matter is, say, half due to neutrinos and half due to cold dark matter (CDM) particles was found viable in connection with violent relaxation [25]. But it does not fit the A1689 cluster. Indeed, heavy particles have a Boltzmann distribution. Being collisionless and relaxed, they are accounted for already by the isothermal galaxy term in Eq. (4) with $\bar{\beta}_G = 1$. So at best they present 1-3% of the A1689 mass, too little for this 50-50 assumption, so it would again imply the unlikely conclusion that this cluster is not representative.

The Tremaine-Gunn argument [26] of no increase of the maximal phase space density (except for a factor 2) is automatically satisfied by the Fermi-Dirac distribution. ³

To describe the dark matter profile of a relaxed galaxy cluster is a clean problem that involves almost no cosmology, so its daring predictions pose a firm confrontation to conclusions based on more intricate cosmological theories, such as the cold dark matter model with cosmological constant (Λ CDM model, concordance model). Indeed, our findings are in sharp contradiction with present cosmological understanding, where neutrinos are believed to be ruled out as major dark matter source [13]. Studies like WMAP5 arrive at bounds of the type $m_{\nu_e} + m_{\nu_\mu} + m_{\nu_\tau} \leq 0.5 \text{ eV}$. They start from the CDM paradigm, or from a mixture of CDM and neutrinos, the reason for this being indirect, namely that without CDM the cosmic microwave background peaks have found no explanation. ⁴ But the CDM particle has not been detected, so other paradigms, such as neutrino dark matter, cannot be dismissed at forehand. The CDM assumption has already questioned [5, 27] and it is also concluded that WIMP dark matter has an eV mass [28].

The common assumption that light (baryons, Lyman- α forest aspects) or intracluster gas trace the local dark matter *density* appears to be invalid, even in the absence of a temperature gradient, for radii at least up to 1.5 Mpc, see fig. 2. Nevertheless, they do trace the enclosed total mass, since this is imposed by hydrostatic equilibrium. The galaxies (G) behave differently from the neutrinos even for $\bar{\beta}_G = 1$, because the first ones are classical while the second ones are degenerate fermions; though non-degenerate, the gas (g) behaves differently from both of them, because it is an ionic mixture with electrons, implying a parameter $\bar{\beta}_g < \bar{\beta}_G$. This non sequitur nullifies many conclusions in literature, notably that sterile neutrinos should have keV mass at least and connections between the Lyman- α forest and local dark matter densities [10, 13, 29].

³Let us answer a criticism often met in literature. Galaxies and dwarf galaxies may have their baryonic dark matter in the form of MACHOs, H-He planets of earth mass [5], thousands of which have been observed [6, 7]. In that scenario the (dwarf) galaxy Tremaine-Gunn bound involves the *proton* mass and is satisfied a million times.

⁴CMB peaks may arise without CDM seeds, namely from viscous instabilities in the baryonic plasma before and at decoupling [5, 7]. Free streaming WIMPs would then not have time enough to wash out the newly created baryonic structures.

As mentioned, active neutrinos alone would bring about half of the expected dark matter. In the early Universe the sterile ones can be created too, at temperatures between 200 and 3.5 MeV, provided neutrinoless double β -decay is possible, a process which violates the lepton number. Neutrinos then are Majorana particles. The related Majorana mass should exceed $m_{\beta\beta} > 10^{-4}$ eV or so, which gracefully respects the experimental upper bound $m_{\beta\beta} < 0.2 - 0.7$ eV [22]. Then $\Omega_\nu \leq 0.19 h_{70}^{-3/2}$.

Both the neutrinos and the antineutrinos fall downwardly in a gravitational field, as usual.

The neutrinos stream freely, cool in expanding space and condense on clusters at $z \sim 28$, forming their dark matter. They simultaneously heat the intracluster gas, which ionizes on its way to the 10 keV virial equilibrium temperature. This makes it plausible that it is the neutrino condensation on clusters that, as a cosmic virial imprint, reionizes all the loosely bound gas, without any need for heavy stars, the currently assumed cause [30].

The central parts of clusters constitute quantum particle structures of several million light years across. We expect that the Universe does not contain larger ones, though we make a reservation for the unknown cause of dark energy.

As usual for clusters, we did not have to invoke a modified Newton dynamics like MOND [31]. The popular NFW mass profile [32] plays no role, since it deals with heavy, non-degenerate dark matter, rather than with degenerate fermions. Fig. 2 shows that the NFW cusp is actually produced by galaxies, classical objects indeed, but not dark.

The cold dark matter paradigm has to be abandoned, a conclusion that was already inferred from observed correlations in galaxy structures [27]. Hot neutrino dark matter has to be reconsidered. A gravitational hydrodynamics theory of top – down large scale structure formation has been proposed more than a decade ago [5].

Our theoretical description of virialized galaxy clusters can be used to process observation data. It can be generalized to hydrostatic equilibrium with temperature profiles. Precise observations of the profiles of the weak lensing, the galaxy velocity dispersion and the X-rays in the relaxed South West region of the Abell 1689 galaxy cluster are welcome. The prediction for the neutrino mass already has a small error and offers, once it is known, a new way to determine the Hubble constant. Simulation of the condensation out of free steaming will test our findings.

As for any physical prediction, the ultimate proof is a direct observation, in our case of the neutrino mass. The Mainz-Troitsk tritium β -decay experiment records the maximal electron energy in the reaction ${}^3\text{H} \rightarrow {}^3\text{He}^+ + e^- + \bar{\nu}_e$, and sets a bound on the electron-antineutrino mass, $m_{\bar{\nu}_e} \leq 2$ eV at the 95% confidence level [33]. This leaves our case viable. The Karlsruhe TRITium Neutrino experiment (KATRIN), scheduled for between 2012 and 2015, will test our prediction by searching for a mass down to 0.2 eV [33], so that our ~ 1.5 eV regime should be relatively easy. A next challenge is to settle the Majorana

mass involved in neutrinoless double β -decay.

The present status of WIMP cold dark matter searches is not good, since none of the many past or current ones has detected the cold dark matter particle ⁵But neither should they still do so if dark matter is just neutrino matter. The benefit of neutrinos over other dark matter candidates is that their existence is beyond any doubt. We have both questioned the reasons to rule them out and derived their mass. They can be dense, in the Abell 1689 center a billion per 5 cc, but they are non-relativistic and annihilate each other too rarely to allow observation of the decay products in sky searches.

* * *

We thank Yu. Baryshev, C. Gibson, R. Schild, R. Balian, J. Smit and J. Kaastra for discussion.

REFERENCES

- [1] J. H. Oort, Bull. Astron. Inst. Netherl. **VI**, 249 (1932).
- [2] F. Zwicky, Helv. Phys. Acta **6**, 110 (1933).
- [3] V. Rubin, N. Thonnard and W. K. Ford, Jr, Astrophys. J. **238**, 471 (1980).
- [4] M. J. Geller and J. P. Huchra, Science **17**, **246** 897 (1989).
- [5] C.H. Gibson, Appl. Mech. Rev. **49**, 299 (1996).
- [6] R. E. Schild, Astrophys. J. **464**, 125 (1996).
- [7] Th. M. Nieuwenhuizen, C.H. Gibson and R. E. Schild, to appear.
- [8] E. Komatsu, et al., Astrophys. J. Suppl. **180**, 330 (2009).
- [9] J. A. Tyson and P. Fischer, Astroph. J. **446**, L55 (1995).
- [10] M. Limousin et al., Astroph. J. **668**, 643 (2007).
- [11] E. W. Kolb and M. S. Turner, *The Early Universe*, (Addison-Wesley, Amsterdam, 1990).
- [12] C. Amsler et al., Phys. Lett. **B667**, 1 (2008).
- [13] J. Lesgourgues and S. Pastor, Phys. Rep. **429**, 307 (2006).
- [14] A. Leonard, et al., Astrophys. J. **666** 51 (2007).
- [15] S. Riemer-Sørensen et al., Astrophys. J. **693**, 1570 (2009).
- [16] K. E. Andersson and G. M. Madejski, Astroph. J. **607**, 190 (2004). The gas mass profile is part of Fig. 9.
- [17] N. Werner et al., Astron. and Astrophys. **482**, L29 (2008).
- [18] D. Lynden-Bell, Mon. Not. Roy. Astron. Soc. **136**, 101 (1967).
- [19] R. Balian and J. P. Blaizot, Am. J. Phys. **67**, 1189 (1999).
- [20] M. C. Gonzalez-Garcia and M. Maltoni, Phys. Rep. **460**,1 (2008).
- [21] J. M. Cline, Phys. Rev. Lett. **68**, 3137 (1992).
- [22] H. V. Klapdor-Kleingrothaus et al., Eur. Phys. J. **A12**, 147 (2001).
- [23] V. Simha and G. Steigman, JCAP **0808**, 011 (2008).
- [24] W. M. Yao et al., J. Phys. **G33**, 1 (2006).
- [25] R. A. Treumann, A. Kull and H. Böhringer, New J. Phys. **2**, 11 (2000).

⁵An incomplete acronym list of WIMP/axion dark matter searches and collaborations is: ADMX, ANAIS, ArDM, ATIC, BPRS, CAST, CDMS, CLEAN, CRESST, CUORE, CYGNUS, DAMA, DEEP, DRIFT, EDELWEISS, ELEGANTS, EURECA, GENIUS, GERDA, GEDEON, GLAST, HDMS, IGEX, KIMS, LEP, LHC, LIBRA, LUX, NAIAD, ORPHEUS, PAMELA, PICASSO, ROSEBUD, SIGN, SIMPLE, UKDM, XENON, XMASS, ZEPLIN.

- [26] S. Tremaine and J. E. Gunn, Phys. Rev. Lett. **42**, 407 (1979).
- [27] M. J. Disney et al., Nature **455**, 1082 (2008).
- [28] C. H. Gibson, J. Fluids Eng. **122**, 830 (2000).
- [29] M. Viel, et al., Phys. Rev. Lett. **97**, 071301 (2006).
- [30] S. Weinberg, *Cosmology*, (Oxford, Oxford, UK, 2008).
- [31] M. Milgrom, Astrophys. J. **270**, 365 (1983).
- [32] J. F. Navarro, C. S. Frenk and S. D. M. White, Astrophys. J. **490**, 493 (1997).
- [33] E. W. Otten and C. Weinheimer, Rep. Prog. Phys **71**, 086201 (2008).